In vivo replacement of damaged bladder urothelium by Wolffian duct epithelial cells

Diya B. Joseph[a], Anoop S. Chandrashekar[a], Lisa L. Abler[a], Li-Fang Chu[b,c], James A. Thomson[b,c], Cathy Mendelsohn[d], and Chad M. Vezina[a,1]

[a]Department of Comparative Biosciences, School of Veterinary Medicine, University of Wisconsin–Madison, Madison, WI 53706; [b]Morgridge Institute for Research, Madison, WI 53715; [c]Department of Cell and Regenerative Biology, University of Wisconsin School of Medicine and Public Health, Madison, WI 53706; and [d]Department of Urology, Columbia University, New York, NY 10032

Edited by Marianne Bronner, California Institute of Technology, Pasadena, CA, and approved July 2, 2018 (received for review February 19, 2018)

The bladder's remarkable regenerative capacity had been thought to derive exclusively from its own progenitors. While examining consequences of DNA methyltransferase 1 (*Dnmt1*) inactivation in mouse embryonic bladder epithelium, we made the surprising discovery that Wolffian duct epithelial cells can support bladder regeneration. Conditional *Dnmt1* inactivation in mouse urethral and bladder epithelium triggers widespread apoptosis, depletes basal and intermediate bladder cells, and disrupts uroplakin protein expression. These events coincide with Wolffian duct epithelial cell recruitment into *Dnmt1* mutant urethra and bladder where they are reprogrammed to express bladder markers, including FOXA1, keratin 5, P63, and uroplakin. This is evidence that Wolffian duct epithelial cells are summoned in vivo to replace damaged bladder epithelium and function as a reservoir of cells for bladder regeneration.

bladder | Wolffian duct | DNMT1 | apoptosis | regeneration

The bladder's specialized epithelium, or urothelium, consists of basal, intermediate, and superficial cell layers which collaborate to establish and maintain a protective barrier against water, ions, and pathogens (1). Uroplakins, expressed on apical surfaces of terminally differentiated superficial cells, form crystalline plaques to establish a permeability barrier. Breach of this barrier exposes bladder mucosa, musculature, and surrounding nerve fibers to urinary irritants, causing pain and voiding dysfunction (2). Although bladder urothelium has a slow turnover rate, it rapidly regenerates in response to injury or infection. Bladder urothelium regenerates from basal and intermediate cell progenitors specified during embryonic development (3–5). There is a clear role for retinoid (5) and other classical developmental signaling pathways (3) in progenitor specification, but the role of epigenetic factors is poorly understood. Highlighting the importance of epigenetics in bladder development, a recent study demonstrated that the Polycomb repressive complex 2, which has histone methyltransferase activity, is essential for maintenance of embryonic and adult urothelial progenitors (6). The initial purpose of this study was to investigate whether DNA methylation is required in lower urinary tract development and specifically in bladder urothelial development. The key maintenance methyltransferase, DNA methyltransferase 1 (*Dnmt1*) coordinates many aspects of organogenesis (7, 8) and maintains progenitors required for tissue regeneration (9). *Dnmt1* is required for progenitor survival, cell differentiation, and lineage commitment in developing intestine (7), retina (10), and pancreas (8), but its requirement in bladder and urethral development has not been examined.

We used a Shh^{cre} (11) driver to conditionally delete *Dnmt1* in embryonic mouse urethral and bladder epithelium, where it is highly expressed (12). Embryonic day (E) 18.5 mutants harbored an abnormally thin bladder urothelium characterized by discontinuous uroplakin expression, fewer basal and intermediate cells, and widespread apoptosis. In earlier developmental stages, *Dnmt1*-depleted urethral and bladder epithelium lost DNA methylation, progressively activated the DNA damage response and P53, and underwent apoptosis at E15.5. By following *Shh* lineage marked cells in urethra and bladder at this stage, our initial focus on DNA methylation gave rise to a far more important discovery: Wolffian duct epithelial cells migrate into the damaged lower urinary tract of mutant mice and reprogram to acquire urethral and bladder epithelial markers (FOXA1, keratin 5, P63, and uroplakin). Our results establish a paradigm for bladder regeneration: Depletion of urothelial progenitors can trigger recruitment of Wolffian duct epithelial cells into the urethra and bladder, where they expand and reprogram to restore the uroplakin barrier. This previously unknown function of Wolffian duct epithelium as a reservoir for bladder-replacing cells has important implications for bladder regenerative therapies.

Results

***Dnmt1* Deletion in *Shh* Lineage Cells Leads to Neonatal Lethality.** Mice carrying one copy of the Shh^{cre} transgene and one copy of a *Dnmt1flox* allele (13) served as experimental controls for mice carrying one copy of the Shh^{cre} allele and two copies of the *Dnmt1flox* allele [*Dnmt1* conditional knockout (*Dnmt1*cKO)]. Initial observation of *Dnmt1*cKO neonates revealed severe lung hypoplasia, cyanosis, and death at postnatal day 0 (*SI Appendix*, Fig. S1 *A* and *B*). Subsequent studies with embryos examined at or before E18.5, before development of respiratory complications, revealed viable *Dnmt1*cKO embryos with a normal

Significance

When the bladder's specialized epithelial lining is damaged by infection or injury, its own basal and intermediate cell progenitors are called upon to restore a functional barrier. Here we show that when these progenitor cells are depleted in conditional *Dnmt1* mutant mice, Wolffian duct epithelial cells migrate into the bladder, acquire bladder epithelial cell characteristics, and restore expression of uroplakin, a critical component of barrier function. This is a demonstration of in vivo replacement of damaged bladder epithelium by nonbladder epithelial cells. The capacity of Wolffian duct epithelial cells to replace damaged urothelium can potentially be leveraged for bladder replacement therapies which are often necessitated in patients with carcinoma or neurogenic bladder.

Author contributions: D.B.J., L.L.A., and C.M.V. designed research; D.B.J., A.S.C., L.-F.C., and C.M.V. performed research; D.B.J., A.S.C., and L.-F.C. analyzed data; and D.B.J., L.L.A., J.A.T., C.M., and C.M.V. wrote the paper.

The authors declare no conflict of interest.

This article is a PNAS Direct Submission.

Data deposition: The data reported in this paper have been deposited in the Gene Expression Omnibus (GEO) database, www.ncbi.nlm.nih.gov/geo (accession no. GSE115477). Raw image files relating to this manuscript have been uploaded to GUDMAP.org Vezina CM (2018) GUDMAP Consortium https://doi.org/10.25548/W-QXXC.

[1]To whom correspondence should be addressed. Email: chad.vezina@wisc.edu.

This article contains supporting information online at www.pnas.org/lookup/suppl/doi:10.1073/pnas.1802966115/-/DCSupplemental.

Published online July 30, 2018.

external appearance and a crown–rump length comparable to controls (*SI Appendix*, Fig. S1*C*). Cre recombination, evaluated by inducible *R26R-LacZ* or *R26R-EYFP* lineage reporters, localized to bladder and urethral epithelium but not caudal Wolffian or Müllerian duct epithelium (Fig. 1*A* and *SI Appendix*, Fig. S3*C*). All subsequent figure panels are from male embryos unless otherwise specified.

Wolffian Duct Epithelial Cells Are Recruited into the *Dnmt1*-Depleted Lower Urinary Tract. We first tested whether DNMT1 protein abundance and global DNA methylation were reduced in E18.5 *Dnmt1*cKO mutants. DNMT1 and 5-methylcytosine (5mC) were not detected in *Shh* lineage ($EYFP^+$) epithelial cells in *Dnmt1*cKO mutants. The most surprising finding was the presence of many $EYFP^-$, $DNMT1^+$, and $5mC^+$ cells in *Dnmt1*cKO urethra and bladder (Fig. 1 *A* and *B* and *SI Appendix*, Fig. S1 *D* and *E*). We used a different lineage reporter (*R26R-LacZ*) to evaluate *Shh* lineage cell distribution. A sizeable cluster of lineage-negative (nonstained with X-Gal) epithelial cells accumulated between the bladder neck and Wolffian duct of *Dnmt1*cKO mutants (Fig. 1 *C* and *D*). Presence of *Shh* lineage-negative cells in this region is unusual, considering that the entire epithelium of the urethra and bladder derives from *Shh* lineage cells (14).

Incomplete Cre-mediated recombination could cause *Shh* lineage-negative cells to accumulate but this is unlikely, given these cells are not randomly distributed but instead restricted to a discrete anatomical region. In addition, 100% Cre recombination was observed in controls (*SI Appendix*, Fig. S1 *F–N*). We then contemplated the unusual possibility that *Shh* lineage-negative cells are recruited to the *Dnmt1*cKO urethra from a different source. The Wolffian duct epithelium, marked by paired box 2 (PAX2) and paired box 8 (PAX8) (15), is the closest nonendodermal epithelial source and derives from a *Shh*-negative lineage (intermediate mesoderm). $PAX2^+$ and $PAX8^+$ cells were restricted to control mouse Wolffian ducts as expected but surprisingly extended into *Dnmt1*cKO urethra and bladder (Fig. 1 *E* and *F*). *Pax2* and *Pax8* mRNAs were expressed in patterns resembling their protein expression (*SI Appendix*, Fig. S2 *A–D*) and we confirmed $PAX8^+$ cells were indeed integrated into the *Dnmt1*cKO urethral epithelium because they were externally bound by a continuous laminin a1 (LAMA1)-stained basement membrane (*SI Appendix*, Fig. S2 *E* and *F*). Collectively, these results support the hypothesis that Wolffian duct epithelial cells are recruited into *Dnmt1*cKO urethra and bladder and that cell recruitment is unidirectional (urethra/bladder epithelial cells do not invade Wolffian duct epithelium). Ureters and Müllerian ducts could be additional sources of $PAX2^+$ and $PAX8^+$ cells but there was no evidence of cell movement from either of these tissues into the urethra and bladder (*SI Appendix*, Fig. S2 *I–L*). Further, when *Dnmt1*cKO bladders are severed from the Wolffian ducts and grafted, no $PAX2^+$ cells appear in bladder (*SI Appendix*, Fig. S2 *M* and *N*).

We examined multiple developmental stages, spanning E12.5–E18.5, to pinpoint when Wolffian duct cells are recruited into *Dnmt1*cKO urethra and bladder. Between E12.5 and E14.5, no $PAX2^+$ Wolffian duct cells were observed in urethra or bladder of either genotype (Fig. 1 *G–J* and *SI Appendix*, Fig. S2 *G* and

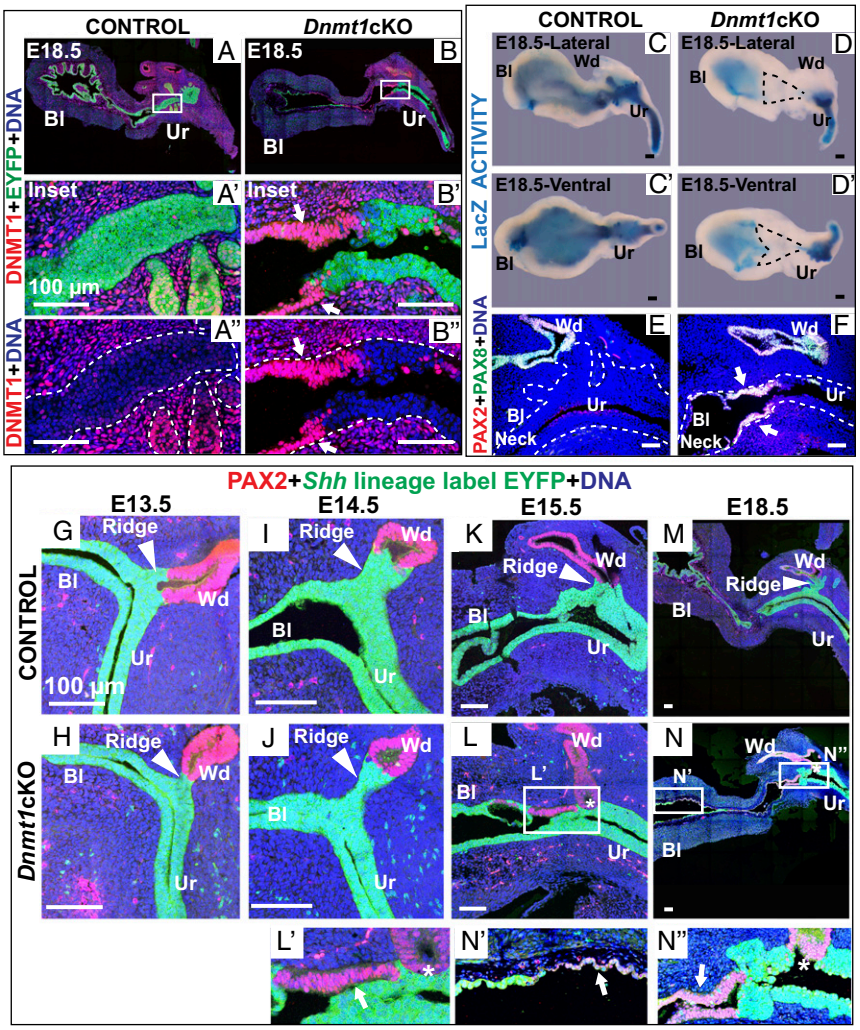

Fig. 1. Wolffian duct-derived epithelial cells are recruited into *Dnmt1* conditional knockout (*Dnmt1*cKO) lower urinary tracts. (*A* and *B*) Lower urinary tract sagittal sections labeled with antibodies against DNMT1 (red) and EYFP (green, labels *Shh* lineage cells). $DNMT1^+$ and $EYFP^-$ cells in *Dnmt1*cKO urethras are indicated by white arrows. Boxed areas in *A* and *B* are magnified in *A′*, *A″*, *B′*, and *B″*. (*C* and *D*) Lateral views and (*C′* and *D′*) ventral views of lower urinary tracts treated with X-Gal to reveal LacZ activity (blue) in *Shh* lineage cells. A wedge of $LacZ^-$ cells is enclosed with black dashed lines. (*E* and *F*) Lower urinary tract sagittal sections labeled with antibodies against Wolffian duct epithelial markers PAX2 (red) and PAX8 (green). $PAX2^+$ and $PAX8^+$ cells in *Dnmt1*cKO UGS epithelium indicated by white arrows. (*G–N*) Lower urinary tract sagittal sections from sequentially staged control and *Dnmt1*cKO embryos labeled with antibodies against PAX2 (red) and EYFP (green, labels *Shh* lineage cells). White arrowheads indicate the UGS ridge and asterisks indicate a deficient UGS ridge in *Dnmt1*cKO embryos. White arrows mark $PAX2^+$ and $EYFP^-$ cells in *Dnmt1*cKO urethra and bladder. DAPI staining is shown in blue. (Scale bar: 100 μm.) Bl, bladder; Bl neck, bladder neck; Ur, urethra; Wd, Wolffian duct.

H). The Wolffian ducts were separated from the urethra and bladder by the urogenital sinus (UGS) ridge, an epithelial thickening on the urethral side of the Wolffian duct–urethra junction. The UGS ridge was present and its size comparable between genotypes at E13.5 and E14.5 (Fig. 1 *G–J*). At E15.5, the *Dnmt1*cKO UGS ridge was smaller than controls and was completely absent by E18.5 (Fig. 1 *K–N*). Wolffian duct cells colonized the male *Dnmt1*cKO urethra at the onset of UGS ridge depletion at E15.5 and progressively expanded into the bladder. None of the ectopic PAX2$^+$ Wolffian duct cells expressed the *Shh* lineage label, indicating these cells do not acquire *Shh* expression or lose DNMT1 within urethra or bladder (*SI Appendix*, Fig. S1 *N* and *O*).

Onset of Wolffian duct cell recruitment at E15.5 excludes the possibility that these cells are remnants of the transitory Wolffian duct derivative, the common nephric duct. The common nephric duct typically recedes at E11.5 (16) and there was no evidence of Wolffian duct cell recruitment into the urethra until E15.5. We also found that Wolffian duct cells are recruited to the female *Dnmt1*cKO urethra at E15.5, before Wolffian duct degradation at E16.5 (*SI Appendix*, Fig. S3), suggesting this phenomenon occurs in both sexes.

Wolffian Duct Cells Recruited to the *Dnmt1*-Depleted Lower Urinary Tract Acquire Bladder Epithelial Characteristics. We found that bladder mesenchyme can instructively reprogram Wolffian duct epithelium when the tissues are combined and grafted under the kidney capsule for continued development (*SI Appendix*, Fig. S4 *G–J*). We tested whether similar reprogramming occurs in Wolffian duct cells recruited to the bladder. During normal development and differentiation, bladder epithelium initially expresses the definitive endoderm marker FOXA1 and then acquires keratin 5 (KRT5), P63, and uroplakin (UPK) to generate basal (KRT5$^+$, P63$^+$, and UPK$^-$), intermediate (KRT5$^-$, P63$^+$, and UPK$^+$), and superficial (KRT5$^-$, P63$^-$, and UPK$^+$) cells (5). During embryonic development in control mice, Wolffian duct epithelium exhibits a columnar morphology in contrast to the cuboidal morphology of urethral epithelium and does not express FOXA1, KRT5, P63, or uroplakins. At the onset of Wolffian duct epithelial cell recruitment into the *Dnmt1*cKO lower urinary tract (E15.5), only a few PAX2$^+$ cells were present in the urethra and these cells expressed FOXA1 but not KRT5 or P63 (*SI Appendix*, Fig. S4 *A–F*). At E18.5, many PAX2$^+$ cells resided in the *Dnmt1*cKO urethra and bladder and all coexpressed FOXA1 (Fig. 2 *A* and *B*). PAX2$^+$ and PAX8$^+$ cells residing closest to the Wolffian duct–urethra junction were KRT5− and P63−, and those in the bladder neck and bladder were KRT5$^+$ and P63$^+$ (Fig. 2 *C–J*). These results indicate that recruited Wolffian duct epithelial cells progressively differentiate as they migrate away from the Wolffian duct and into bladder. Consistent with this hypothesis, recruited Wolffian duct cells near the E18.5 *Dnmt1*cKO Wolffian duct had a columnar morphology resembling Wolffian duct epithelia, while those in the bladder had a cuboidal morphology resembling bladder epithelia (Fig. 2*O*).

Cell counts show that 100% of Wolffian duct cells (*Shh* lineage negative) in the urethra express PAX2, whereas only 64% of Wolffian duct cells in the bladder express PAX2 (346/537 cells counted) (*SI Appendix*, Fig. S1*N*). We hypothesized that Wolffian duct cells enter the bladder from the urethra as a homogenous population and some lose PAX2 expression upon differentiation. We tested and confirmed that bladder-recruited Wolffian duct cells (*Shh* lineage negative, EYFP$^-$ cells) achieved expression of UPK, the defining marker of bladder superficial cells (Fig. 2 *P* and *Q*). Interestingly, these UPK$^+$ Wolffian duct cells appeared to be PAX8$^-$ (Fig. 2 *K–N*), although adjacent basal cells were PAX8$^+$. We interpret these results as evidence that Wolffian duct cells partially retain their identity when reprogrammed to basal cells but lose their Wolffian duct identity when reprogrammed to superficial cells.

***Dnmt1*-Depleted Lower Urinary Tract Epithelia Differentiate Inappropriately and Are Abnormally Thin.** Having characterized Wolffian duct cell recruitment and reprogramming in *Dnmt1*cKO lower urinary tracts, we turned our attention to the *Dnmt1*-depleted epithelium into which they are recruited. *Dnmt1*cKO urethras exhibited abnormal dorsal–ventral patterning and disorganization, with acellular holes in the epithelium (Fig. 3 *A–F*). *Dnmt1*cKO bladders were abnormally large, filled with urine (*SI Appendix*, Fig. S5 *A* and *B*), and featured a thinner epithelium than controls (Fig. 3 *G–I*).

We hypothesized *Dnmt1* deficiency causes inappropriate epithelial differentiation and cell depletion, creating a permissive environment for colonization by Wolffian duct cells. We focused on the bladder apex region because it is the least contaminated by recruited Wolffian duct cells (Fig. 1 *A* and *B*) and made three observations supporting inappropriate differentiation of *Dnmt1*-depleted bladder epithelial cells. First, we noted a precocious appearance of KRT5$^+$ and P63$^+$ basal epithelial cells in E15.5 *Dnmt1*cKOs compared with controls (Fig. 3 *J*, *K*, and *R* and *SI Appendix*, Fig. S5*I*). Second, E18.5 *Dnmt1*cKO bladders had fewer KRT5$^+$ and P63$^+$ basal cells than controls and were characterized by weak and discontinuous UPK expression, consistent with impaired barrier function (Fig. 3 *L–O* and *R*). Third, E18.5 *Dnmt1*cKO bladder cells ectopically expressed the squamous epithelial marker keratin 17 (KRT17) (6), which was absent in control bladder cells (Fig. 3 *P* and *Q*) and Wolffian duct-derived bladder epithelium (*SI Appendix*, Fig. S6 *Q–T*). The proportion of basal, intermediate, and superficial cells in *Dnmt1*cKO bladder epithelium was also different from controls (Fig. 3*R*). An increased frequency of superficial cells at the expense of basal and intermediate populations supports the hypothesis that *Dnmt1* deficiency drives premature cell differentiation and depletes bladder progenitors. Bladder development is dependent on reciprocal signaling between the epithelium and mesenchyme. Non-cell autonomous effects of epithelial DNMT1 deletion were observed in *Dnmt1*cKO bladder mesenchyme, including reduced lamina propria cell density and decreased COL1A1 expression (*SI Appendix*, Fig. S5 *C–H*). The expression profile of Wolffian duct-derived bladder epithelium closely resembled control bladder urothelium but the proportion of bladder epithelial subtypes was changed (*SI Appendix*, Fig. S6). UPK staining was discontinuous where *Dnmt1* was depleted (EYFP$^+$) but continuous where Wolffian duct cells (EYFP$^-$) replaced the damaged epithelium (*SI Appendix*, Figs. S6 *U–X* and S7). This is evidence that recruited Wolffian duct cells not only differentiate toward a bladder fate, but also restore the UPK barrier.

***Dnmt1*-Depleted Lower Urinary Tract Cells Are Hypomethylated and Undergo Apoptosis.** To understand the mechanisms underlying epithelial depletion and disorganization, we performed RNA-sequencing (RNA-Seq) analysis of isolated E15.5 bladder epithelium (at onset of Wolffian duct migration). We observed increased abundance of P53 targets, including *Cdkn1a1*, *Ccng1*, and *Pmaipi1* (*Noxa*) (*SI Appendix*, Fig. S8). Previous studies in developing intestine and pancreas associated *Dnmt1* depletion with DNA hypomethylation and P53-mediated apoptosis characterized by gamma-H2AX activation (DNA damage marker), P53 activation (Ser15 phosphorylation), and caspase 3 cleavage (7, 8). We examined whether a similar series of events precipitates apoptosis of *Dnmt1*cKO urethra and bladder epithelium. Loss of DNMT1 protein and 5mC labeling was detected as early as E13.5 in *Dnmt1*cKO urethra and bladder (*SI Appendix*, Fig. S9 *A–D*). Immunolabeling showed that phospho-gamma-H2AX (Fig. 4 *A–H*) and phospho-P53 Ser15 (Fig. 4 *I–P*) were increased in *Dnmt1*cKO urethra and bladder starting at least as early as E13.5. Phospho-P53 Ser15 appeared to localize to mitochondria, was restricted to *Dnmt1*-depleted (EYFP$^+$) cells, and was absent from recruited Wolffian duct cells (EYFP$^-$) (*SI Appendix*, Fig. S9 *E–P*).

We next tested whether DNA damage and P53 phosphorylation triggered apoptosis in *Dnmt1*cKO epithelial cells. Cleaved

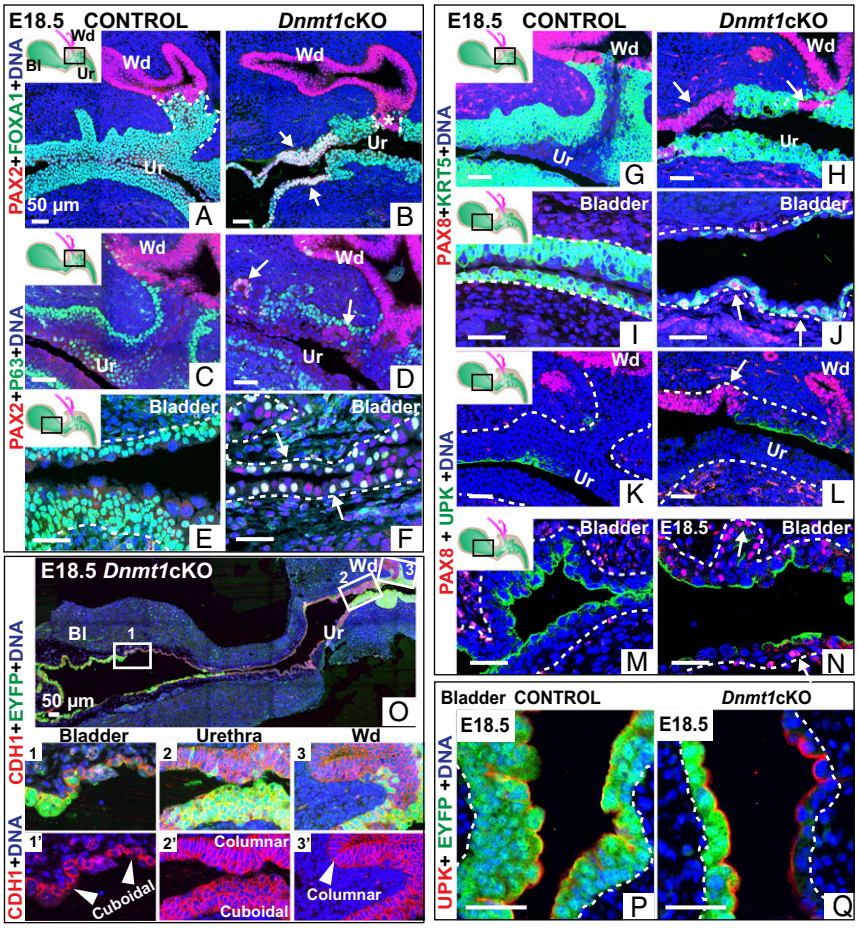

Fig. 2. Recruited Wolffian duct cells acquire bladder characteristics as they expand into the *Dnmt1*cKO urethra and bladder. E18.5 male lower urinary tract sagittal sections labeled with antibodies against (*A* and *B*) FOXA1 (green) and PAX2 (red, labels Wolffian duct epithelium), (*C*–*F*) PAX2 (red) and P63 (green, labels basal epithelium), (*G*–*J*) PAX8 (red, labels Wolffian duct epithelium) and KRT5 (green, labels basal epithelium), and (*K*–*N*) PAX8 (red) and UPK (green, labels superficial epithelium). White arrows indicate $PAX2^+$ or $PAX8^+$ cells in *Dnmt1*cKO urethra and bladder epithelia. The anatomical region shown in each panel (urethra or bladder) is depicted in the schematic diagram. (*O*) E18.5 male *Dnmt1*cKO lower urinary tract labeled with CDH1 (red, labels epithelial cells) and EYFP (green, labels *Shh* lineage cells). (*P* and *Q*) E18.5 bladder sections labeled with antibodies against UPK (red) and EYFP (green). White dotted lines mark the bladder epithelial–stromal interface. DAPI staining is shown in blue. (Scale bar: 50 μm.) Bl, bladder; Bl neck, bladder neck; Ur, urethra; Wd, Wolffian duct.

caspase 3-positive lower urinary tract epithelial cells were rare and their frequency did not differ between genotypes at E13.5 and E14.5 (Fig. 4 *Q*–*T*). By E15.5 and continuing through E18.5, cleaved caspase 3-positive epithelial cells were significantly more frequent in *Dnmt1*cKOs than controls (Fig. 4 *U*–*Z*). Cleaved caspase 3 staining in *Dnmt1*cKOs was confined to *Dnmt1*-depleted *Shh* lineage ($EYFP^+$) cells and was absent from recruited Wolffian duct ($EYFP^-$) cells (*SI Appendix*, Fig. S10). Thus, DNA hypomethylation, DNA damage, and P53 activation precede apoptosis in *Dnmt1*cKO urethra and bladder epithelia at E15.5, and apoptosis coincides with Wolffian duct cell recruitment. Because Wolffian duct cells are not recruited into the lower urinary tract until *Dnmt1*-deficient cells undergo apoptosis, we conclude Wolffian duct cell recruitment is a consequence of *Dnmt1* ablation.

Discussion

Our results support the model in Fig. 5. *Dnmt1* ablation in urethral and bladder epithelium causes global DNA hypomethylation, initiates a DNA damage response, and drives P53-mediated apoptosis. Urethral and bladder epithelial cell depletion and UGS ridge breakdown are triggers for Wolffian duct cell recruitment. Recruited cells migrate into the bladder, acquire bladder-specific markers, and restore the bladder's uroplakin barrier. These results identify Wolffian duct epithelium as a reservoir for bladder epithelial cell replacement.

This study investigates the role of DNMT1 in urethral and bladder development. *Dnmt1* deletion in the lower urinary tract caused extensive epithelial damage as evidenced by acellular holes in the epithelium, increased frequency of apoptotic cells, thinning of bladder epithelium, and discontinuous uroplakin staining. DNA hypomethylation is accompanied by activation of the DNA damage response, P53 accumulation, and apoptosis. The sequence of molecular events leading to *Dnmt1*-deficient bladder cell apoptosis matches that described in *Dnmt1* depletion studies in the developing intestine (7) but the outcome is unique: *Dnmt1* ablation in lower urinary tract epithelium triggers cell movement events that were not detected in previous conditional *Dnmt1* mutant studies. Together, our results demonstrate a requirement for *Dnmt1* in maintaining global DNA methylation, progenitor cell survival, and appropriate differentiation of developing bladder epithelia.

Early in embryonic development, Wolffian ducts elongate along the anteroposterior axis, turn toward the midline, and fuse with the cloacal epithelium (precursor of urethral and bladder epithelia). The timing of Wolffian duct–urethra junction formation is critical and the mechanism has been thoroughly characterized (17), but it was not known how this junction is maintained during lower urinary tract development and maturation. Our study reveals an unexpected role of *Dnmt1* in maintaining the junction by preventing the intermixing of Wolffian duct and urethral cells. Although the Wolffian duct–urethra junction is formed normally in *Dnmt1* mutants, it is not maintained. We have demonstrated that the Wolffian duct–urethral junction can be destabilized and breached by epithelial depletion/injury of the urethral epithelium. Other instances of epithelial injury to the urethra could potentially cause this to happen in humans.

Wolffian duct cell recruitment into the urethra and bladder is an unprecedented observation, but we only examined embryonic stages due to neonatal lethality of *Dnmt1*cKO mutants. Our results raise questions about whether postnatal Wolffian duct derivatives (vas deferens, seminal vesicle) retain the capacity to invade the postnatal urethra and bladder. Intriguing support for this possibility exists in patients with the rare condition of

DEVELOPMENTAL BIOLOGY

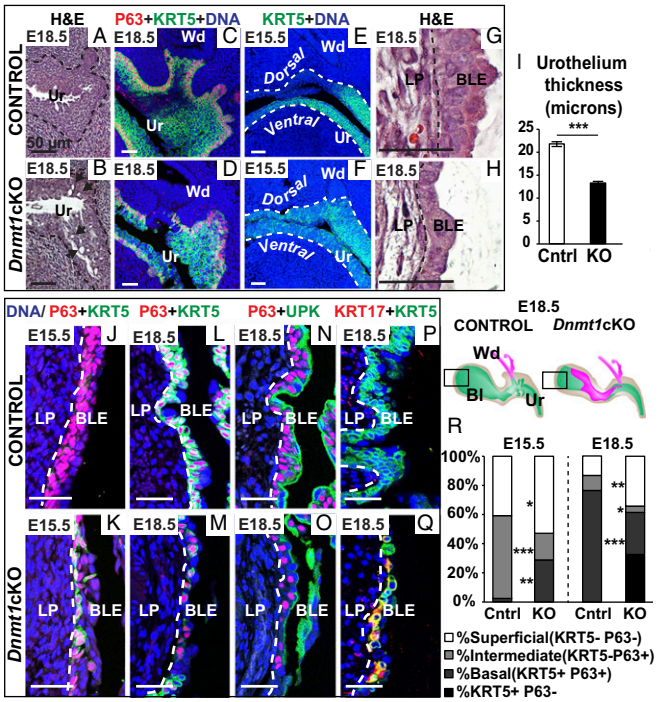

Fig. 3. *Dnmt1*-depleted lower urinary tract epithelial cells precociously differentiate and disorganize beginning at E15.5. (*A* and *B*) H&E stained E18.5 urethral sections. Black arrows indicate acellular holes in *Dnmt1*cKO urethral epithelium. (*C* and *D*) E18.5 urethral sections labeled with basal markers KRT5 (green) and P63 (red). (*E* and *F*) E15.5 urethra sections labeled with KRT5 (green). (*G* and *H*) H&E-stained E18.5 bladder sections used to quantify (*I*) bladder epithelial thickness. (*J* and *K*) E15.5 bladder sections stained with antibodies against P63 (red) and KRT5 (green). E18.5 bladder sections from region depicted in diagram stained with (*L* and *M*) P63 (red) and KRT5 (green), (*N* and *O*) P63 (red) and UPK (green), or (*P* and *Q*) KRT17 (red) and KRT5 (green). (*R*) Percentages of basal, intermediate, and superficial bladder epithelial cells at E15.5 and E18.5. Dashed lines demarcate the epithelial–mesenchymal interface. DAPI staining is shown in blue. (Scale bar: 50 μm.) Graphical data are reported as mean ± SEM of at least three male mice per genotype. Student's *t* test $*P < 0.05$, $**P < 0.01$, $***P < 0.001$. Bl, bladder; Bl neck, bladder neck; BLE, bladder epithelium; Cntrl, control; KO, *Dnmt1*cKO; LP, lamina propria; Ur, urethra; Wd, Wolffian duct.

nephrogenic adenoma, a benign lesion of the bladder or urethra observed most frequently in patients with a history of bladder injury, inflammation, infection, kidney stones, or urogenital surgeries (18, 19). Presence of PAX2- and PAX8- immunopositive cells in bladder and urethral biopsies is diagnostic for nephrogenic adenoma (20), but the source of these cells is not completely known. One study demonstrated that exfoliated kidney epithelial cells from donors colonize bladders of kidney transplant recipients who later developed nephrogenic adenoma (18). Whether other cell types, including Wolffian duct epithelium, can also be recruited to the postnatal bladder has not been examined. The adult regenerative capacity of Wolffian duct derivatives is an important avenue to pursue. Our study and nephrogenic adenoma demonstrate the ability of injured bladder epithelium to recruit nonbladder cells to repair itself. These nonbladder cells could behave differently from normal bladder epithelium in disease contexts and could contribute to disease in the long term.

One of the most surprising observations from this study is the newly recognized capacity of mesodermal Wolffian duct epithelial cells to acquire endodermal bladder epithelial characteristics after invading *Dnmt1*cKO bladder epithelium. Tissue recombination studies using in vivo grafting of tissue recombinants have identified the inductive capacities of embryonic bladder mesenchyme. Embryonic bladder mesenchyme induces urothelial differentiation when recombined with adult bladder epithelium (21) or adult mesenchymal stem cells (22), and we report here that the bladder mesenchyme can instructively reprogram Wolffian duct epithelium. The presence of Wolffian duct epithelial cells in the inductive bladder mesenchyme niche of *Dnmt1*cKO mutants provides a unique opportunity to study Wolffian duct epithelial reprogramming by bladder mesenchyme in vivo. Once in the bladder, recruited Wolffian duct epithelial

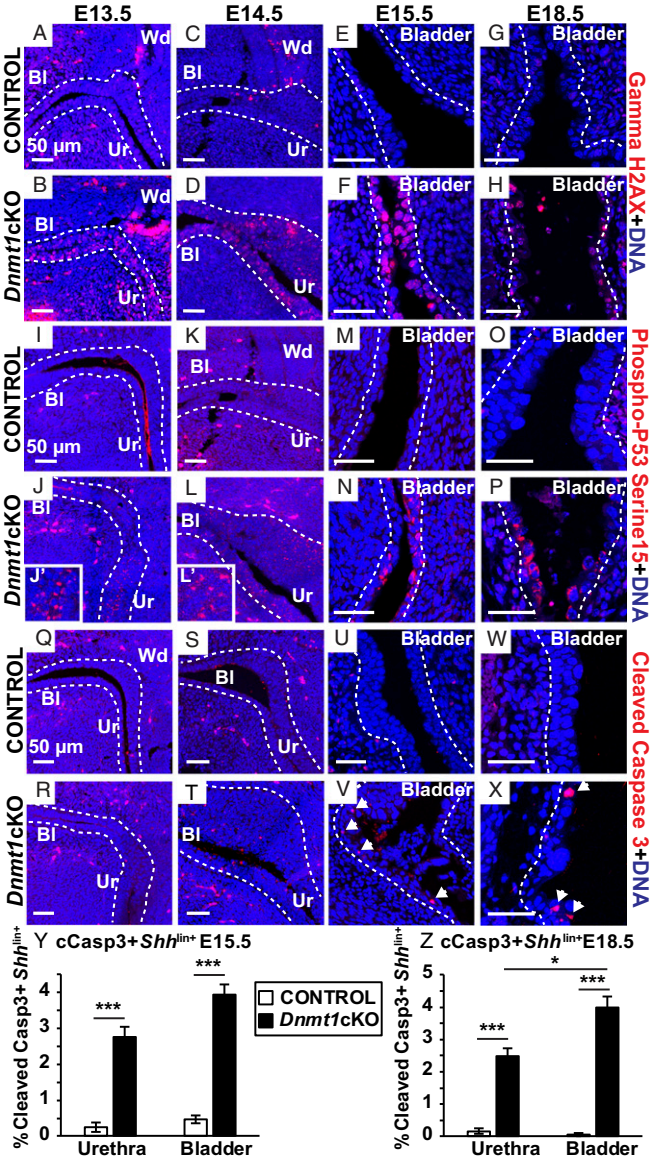

Fig. 4. Hypomethylation triggers DNA damage and P53-mediated apoptosis in *Dnmt1*cKO urethra and bladder. E13.5–E18.5 lower urinary tract sections were labeled with antibodies against: (*A–H*) gamma-H2AX (red, marker of DNA damage response) and (*I–P*) phospho-P53 serine 15 (red, marks active P53). *J*′ and *L*′ are magnified regions from *J* and *L*. (*Q–X*) Cleaved caspase 3 (red, marks apoptotic cells) and EYFP (*Shh* lineage label, not shown to better visualize red labeling). Percentage of cleaved caspase 3^+ *Shh* lineage cells was determined at (*Y*) E15.5 and (*Z*) E18.5. White arrows indicate apoptotic cells. White dashed lines demarcate the epithelial–mesenchymal interface. DAPI staining is shown in blue. (Scale bar: 50 μm.) Graphical data are reported as mean ± SEM of at least three male mice per genotype. Student's *t* test $*P < 0.05$, $***P < 0.001$. Bl, bladder; Bl neck, bladder neck; Ur, urethra; Wd, Wolffian duct.

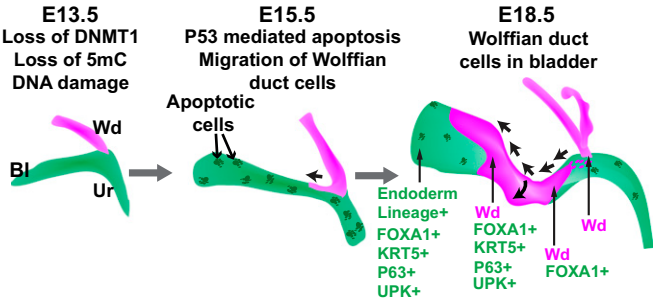

Fig. 5. Model of Wolffian duct cell recruitment and reprogramming in *Dnmt1*cKO mice.

cells acquire expression of KRT5, P63, and uroplakin, signifying urothelial differentiation. Progressive differentiation of recruited Wolffian duct cells as they move from urethra to bladder suggests that the degree of reprogramming could depend on the time spent in the new niche or relative location within this niche.

Bladder basal and intermediate cells had been considered the only populations to participate in bladder regeneration after injury (4, 5). Here we demonstrate that Wolffian duct epithelial cells can also repopulate injured bladders and restore a uroplakin barrier. This capacity can potentially be leveraged for bladder regeneration therapies. Currently, intestinal epithelium is used as a source of tissue for creating neobladders for urine repositories. However, disparate functions of intestinal and bladder epithelium lead to complications, which include excess mucous production that increases urine viscosity and impairs neobladder emptying (23). Alternate strategies for bladder replacement include the use of acellular matrices as scaffolds to guide regeneration (24). Our results support the possibility that Wolffian duct-derived tissue may be another cell source for autologous bladder regeneration. Crucial to future studies is a determination of whether Wolffian duct derivatives retain the capacity to reprogram into bladder epithelial cells during postnatal stages or in adulthood.

Methods

Data Dissemination. To increase rigor, reproducibility, and transparency, raw image files and other data generated as part of this study were deposited into the GUDMAP consortium database and are fully accessible at: https://doi.org/10.25548/W-QXXC (25).

Conditional *Dnmt1* Mutants. Mice were housed as previously described (26). All procedures performed on mice were approved by the University of Wisconsin–Madison Animal Care and Use Committee and were carried out in accordance with the Guide for the Care and Use of Laboratory Animals. *Shh*^{cre} alleles (B6.Cg*Shh*$^{tm1(EGFP/cre)Cjt/J}$) (11) were used to conditionally inactivate *Dnmt1* using *Dnmt1flox* alleles (B6.129S4-*Dnmt1*$^{tm2Jae/Mmucd}$) in *Shh* lineage cells marked with *R26R-LacZ* (27) or *R26R-EYFP* (28) reporter alleles. Of the embryos generated by timed matings, *Shhcre/+; Dnmt1flox/+; R26R/+* embryos (control) were used as controls and compared with age-matched mutant littermates of the genotype *Shhcre/+; Dnmt1flox/flox; R26R/+* (*Dnmt1*cKO).

Phenotype Analysis. β-Galactosidase (LacZ) activity assay (29), fluorescent immunohistochemistry (30), and in situ hybridization on tissue sections (31) were performed as described previously. For hematoxylin–eosin (H&E) staining, nuclei were stained with hematoxylin QS (Vector Laboratories) and counterstained with 0.25% eosin. Information about antibodies and PCR-generated riboprobes used in this study are provided in *SI Appendix*.

Statistical Analysis. Homogeneity of variance was determined using Bartlett's test or Levene's test packages for R. Student's *t* test or ANOVA was performed on parametric data. Results are presented as mean ± SEM (SEM) for at least three litter independent male or female embryos per genotype. *P* values <0.05 were considered significant.

See *SI Appendix* for extended methods.

ACKNOWLEDGMENTS. We thank members of the C.M.V. laboratory for technical assistance, and Dr. Robert Lipinski and Caden Ulschmid (University of Wisconsin–Madison) and Dr. Xin Sun (University of California, San Diego) for critical insights, and Dr. Xin Sun for providing mice. This work is supported by National Institutes of Health Grants R01 DK099328, U54 DK104310, U01 DK110807 (to C.M.V.), and U54 DK104309 and R01 DK095044-03 (to C.M.).

1. Georgas KM, et al. (2015) An illustrated anatomical ontology of the developing mouse lower urogenital tract. *Development* 142:1893–1908.
2. Khandelwal P, Abraham SN, Apodaca G (2009) Cell biology and physiology of the uroepithelium. *Am J Physiol Renal Physiol* 297:F1477–F1501.
3. Shin K, et al. (2011) Hedgehog/Wnt feedback supports regenerative proliferation of epithelial stem cells in bladder. *Nature* 472:110–114.
4. Papafotiou G, et al. (2016) KRT14 marks a subpopulation of bladder basal cells with pivotal role in regeneration and tumorigenesis. *Nat Commun* 7:11914.
5. Gandhi D, et al. (2013) Retinoid-signaling in progenitors controls specification and regeneration of the urothelium. *Dev Cell* 26:469–482.
6. Guo C, Balsara ZR, Hill WG, Li X (2017) Stage- and subunit-specific functions of polycomb repressive complex 2 in bladder urothelial formation and regeneration. *Development* 144:400–408.
7. Elliott EN, Sheaffer KL, Schug J, Stappenbeck TS, Kaestner KH (2015) Dnmt1 is essential to maintain progenitors in the perinatal intestinal epithelium. *Development* 142:2163–2172.
8. Georgia S, Kanji M, Bhushan A (2013) DNMT1 represses p53 to maintain progenitor cell survival during pancreatic organogenesis. *Genes Dev* 27:372–377.
9. Sen GL, Reuter JA, Webster DE, Zhu L, Khavari PA (2010) DNMT1 maintains progenitor function in self-renewing somatic tissue. *Nature* 463:563–567.
10. Nasonkin IO, et al. (2013) Conditional knockdown of DNA methyltransferase 1 reveals a key role of retinal pigment epithelium integrity in photoreceptor outer segment morphogenesis. *Development* 140:1330–1341.
11. Harfe BD, et al. (2004) Evidence for an expansion-based temporal Shh gradient in specifying vertebrate digit identities. *Cell* 118:517–528.
12. Keil KP, et al. (2013) Catalog of mRNA expression patterns for DNA methylating and demethylating genes in developing mouse lower urinary tract. *Gene Expr Patterns* 13:413–424.
13. Jackson-Grusby L, et al. (2001) Loss of genomic methylation causes p53-dependent apoptosis and epigenetic deregulation. *Nat Genet* 27:31–39.
14. Seifert AW, Harfe BD, Cohn MJ (2008) Cell lineage analysis demonstrates an endodermal origin of the distal urethra and perineum. *Dev Biol* 318:143–152.
15. Bouchard M, Souabni A, Mandler M, Neubüser A, Busslinger M (2002) Nephric lineage specification by Pax2 and Pax8. *Genes Dev* 16:2958–2970.
16. Batourina E, et al. (2005) Apoptosis induced by vitamin A signaling is crucial for connecting the ureters to the bladder. *Nat Genet* 37:1082–1089.
17. Chia I, et al. (2011) Nephric duct insertion is a crucial step in urinary tract maturation that is regulated by a Gata3-Raldh2-Ret molecular network in mice. *Development* 138:2089–2097.
18. Mazal PR, et al. (2002) Derivation of nephrogenic adenomas from renal tubular cells in kidney-transplant recipients. *N Engl J Med* 347:653–659.
19. Ford TF, Watson GM, Cameron KM (1985) Adenomatous metaplasia (nephrogenic adenoma) of urothelium. An analysis of 70 cases. *Br J Urol* 57:427–433.
20. Piña-Oviedo S, Shen SS, Truong LD, Ayala AG, Ro JY (2013) Flat pattern of nephrogenic adenoma: Previously unrecognized pattern unveiled using PAX2 and PAX8 immunohistochemistry. *Mod Pathol* 26:792–798.
21. Oottamasathien S, et al. (2006) Bladder tissue formation from cultured bladder urothelium. *Dev Dyn* 235:2795–2801.
22. Anumanthan G, et al. (2008) Directed differentiation of bone marrow derived mesenchymal stem cells into bladder urothelium. *J Urol* 180(Suppl):1778–1783.
23. N'Dow J, Robson CN, Matthews JN, Neal DE, Pearson JP (2001) Reducing mucus production after urinary reconstruction: A prospective randomized trial. *J Urol* 165:1433–1440.
24. Lin HK, et al. (2015) Biomatrices for bladder reconstruction. *Adv Drug Deliv Rev* 82–83:47–63.
25. Vezina CM (2018) GUDMAP Consortium. Available at https://doi.org/10.25548/W-QXXC. Accessed July 19, 2018.
26. Mehta V, et al. (2011) Atlas of Wnt and R-spondin gene expression in the developing male mouse lower urogenital tract. *Dev Dyn* 240:2548–2560.
27. Soriano P (1999) Generalized lacZ expression with the ROSA26 Cre reporter strain. *Nat Genet* 21:70–71.
28. Srinivas S, et al. (2001) Cre reporter strains produced by targeted insertion of EYFP and ECFP into the ROSA26 locus. *BMC Dev Biol* 1:4.
29. Cheng TC, Wallace MC, Merlie JP, Olson EN (1993) Separable regulatory elements governing myogenin transcription in mouse embryogenesis. *Science* 261:215–218.
30. Abler LL, et al. (2011) A high-resolution molecular atlas of the fetal mouse lower urogenital tract. *Dev Dyn* 240:2364–2377.
31. Abler LL, et al. (2011) A high throughput in situ hybridization method to characterize mRNA expression patterns in the fetal mouse lower urogenital tract. *J Vis Exp,* 2912.